High-Performance Microwave Coplanar Bandpass and Bandstop Filters on Si Substrates

K. T. Chan, Albert Chin, *Senior Member, IEEE*, Ming-Fu Li, *Senior Member, IEEE*, Dim-Lee Kwong, *Senior Member, IEEE*, Sean P. McAlister, *Senior Member, IEEE*, D. S. Duh, W. J. Lin, and C. Y. Chang

***Abstract*—High-performance bandpass and bandstop microwave coplanar filters, which operate from 22 to 91 GHz, have been fabricated on Si substrates. This was achieved using an optimized proton implantation process that converts the standard low-resistivity (∼10 Ω · cm) Si to a semi-insulating state. The bandpass filters consist of coupled lines to form a series resonator, while the bandstop filter was designed in a double-folded short-end stub structure. For the bandpass filters at 40 and 91 GHz, low insertion loss was measured, close to electromagnetic simulation values. We also fabricated excellent bandstop filters with very low transmission loss of ∼1 dB and deep band rejection at both 22 and 50 GHz. The good filter performance was confirmed by the higher substrate impedance to ground, which was extracted from the well-matched S-parameter equivalent-circuit data.**

***Index Terms*—Bandpass, bandstop, filter, integration, millimeter wave, Si.**

I. Introduction

THE concept of integrating filters with CMOS monolithic microwave integrated circuits (MMICs) on silicon (Si) substrates [1]–[3] is appealing because of lower cost and compact system considerations [4]. This requirement becomes even more urgent as the operation frequency of Si communication integrated circuits (ICs) increases. However, the performance of microwave filters integrated on Si suffers from the high RF loss and crosstalk of the low-resistivity (10 Ω · cm) Si substrates [5]–[12], as does the quality of inductors and transmission lines on Si. This is the fundamental limitation of Si-based RF circuits, even using advanced Si-on-insulator (SOI) technology. Several methods have been proposed including using porous Si fabricated by anodic etching [11] or microelectromechanical system (MEMS) technology [1], [12], but these nonconventional very large scale integration (VLSI) technologies face additional process integration issues and packaging challenges. To overcome this problem, we have previously developed an ion-implantation technology that can convert conventional Si substrates (10 Ω · cm) to a semi-insulating state (∼10^6 Ω · cm) [5]–[10]. Good performance has been realized for an integrated bandpass filter on Si up to 40 GHz [10]. In this paper, we extend the operation frequency of the bandpass filter into the W-band and also investigate microwave bandstop filters. The ion implantation was optimized for better compatibility with current VLSI processes. Using this modified technology, we have achieved excellent RF performance, close to the ideal electromagnetic (EM) simulations, for both coplanar bandpass and bandstop filters from 22 to 91 GHz. These excellent results suggest that the microwave coplanar filters can be integrated into CMOS MMICs on Si substrates, for single chip radio applications, using the simple ion-implantation process.

Manuscript received January 16, 2003; revised April 10, 2003. This work was supported in part by the National Science Council under Grant 90-2215-E-009-044 and under the National Research Council of Canada–National Science Council Collaborative Program.

K. T. Chan and A. Chin are with the Department of Electronics Engineering, National Chiao Tung University, Hsinchu, Taiwan 30050, R.O.C. (e-mail: achin@cc.nctu.edu.tw).

M.-F. Li is with the Silicon Nano Device Laboratory, Department of Electrical and Computer Engineering, National University of Singapore, Singapore 119260.

D.-L. Kwong is with the Department of Electrical and Computer Engineering, The University of Texas, Austin, TX 78752 USA.

S. P. McAlister is with the National Research Council of Canada, Ottawa, ON, Canada K1A 0R6.

D. S. Duh and W. J. Lin are with the Institute of Nuclear Energy Research, Taoyuan, Taiwan 32547, R.O.C.

C. Y. Chang is with the Department of Communication Engineering, National Chiao Tung University, Hsinchu, Taiwan 30010, R.O.C.

Digital Object Identifier 10.1109/TMTT.2003.815890

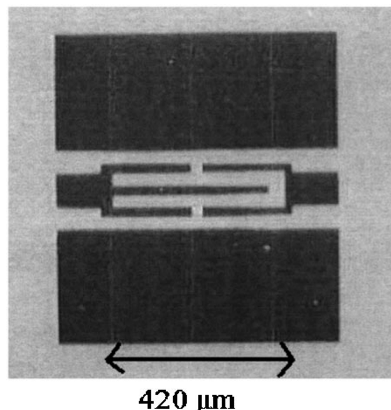

Fig. 1. Photographic image of the fabricated bandpass filters designed for the W-band of ∼94 GHz. The dark area in the photograph is metal pattern. The total length is 620 μm, while the central conductor has a length $\sim \lambda_g/2$.

II. Filter Design and Fabrication

The filters were designed using the EM simulation software *IE3D*. A coplanar waveguide (CPW) structure was used for the filter design since it can be well integrated into existing RF ICs on Si substrates without the need for incorporating via-holes. For the design of microwave components, the CPW structure is less sensitive to the substrate thickness and substrate dielectric constant than microstrip structures. The filters have 50-Ω input impedance with 150-μm ground–signal–ground (GSG) coplanar transmission lines for good RF impedance matching. Fig. 1 shows a photographic image of the fabricated W-band

0018-9480/03$17.00 © 2003 IEEE

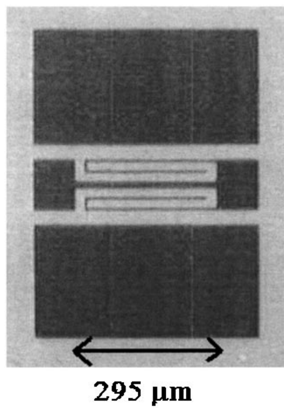

Fig. 2. Image of the fabricated bandstop filters designed for 52 GHz. The dark area in the photograph is metal pattern. The total length is 495 μm, while the folded structure reduces the slot length to $\sim \lambda_g/8$. (A bandstop filter with a 22-GHz center frequency was also designed and studied.)

bandpass filters. Here, the values of the equivalent capacitance and inductance depend on the gap spacing between the coplanar couple lines and the width of the central line. The total filter length is approximately $\lambda/2$ with each stub finger 25-μm wide. The fabricated bandstop filter is shown in Fig. 2. The width of the central conductor is 20 μm and each stub width is 10 μm with a gap of 15 μm. At resonant frequencies, the inner $\lambda/4$ slots transfer the equivalent open circuit to a short circuit, thus, a bandstop response was obtained [1], [2]. The bandstop filter has a double-folded short-end stub form, which reduces the filter size from $\lambda_g/4$ to $\lambda_g/8$ by folding stubs and slots in the filter structure [1], [2].

The filters were fabricated on SiO_2/Si substrates by patterning a 4-μm-thick Al metal layer deposited on the 1.5-μm-thick SiO_2 layer already grown for better substrate isolation. An improved ~4-MeV proton implantation scheme [5]–[10] was performed after the filter fabrication. This avoids potential contamination to the VLSI process line and uses a commercial thick photoresist. It is important to notice that the unmasked MOSFET and capacitor will fail due to the damage to the dielectric layer by proton implantation [6]. Therefore, the thick photoresist in combination of optimized energy are the key factors to realize an integrated single-chip radio. Fabricated filters were characterized using an HP 8510C Network Analyzer and a probe station up to 110 GHz without any deembedding procedure.

III. Results and Discussion

A. Transmission Line

Since the substrate RF loss is a key factor for filters, we first discuss the RF loss in proton-implanted transmission lines. Fig. 3 shows the measured and simulated power loss of 1000-m-long CPW transmission lines up to 110 GHz with or without the proton implantation. The optimized proton-implantation process, performed after the wafer processing, significantly reduces the RF loss from the Si substrates, keeping it at less than 0.6 dB and up to 110 GHz. This excellent microwave performance is close to the ideal *IE3D* simulation results for transmission lines on semi-insulating Si with resistivity of 1 M $\cdot$ cm used in *IE3D*. The small increasing loss with increasing frequency for transmission lines with implantation is believed to be due to the conductor loss, but has only a weak effect on filter performance, as will be shown below. The modified proton implantation process can also be used for microwave filters integrated on Si.

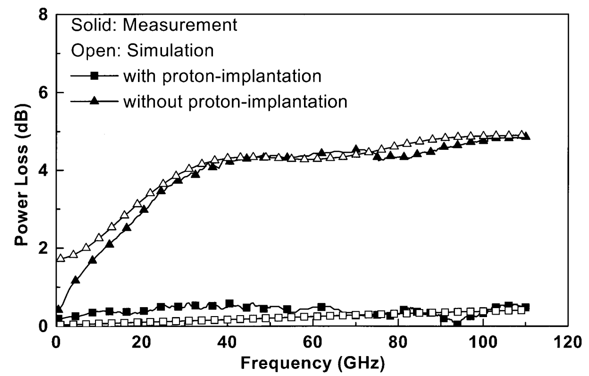

Fig. 3. Measured and simulated power loss for 1-mm-long CPW transmission lines fabricated on 1.5-μm SiO_2/Si substrates with or without proton implantation.

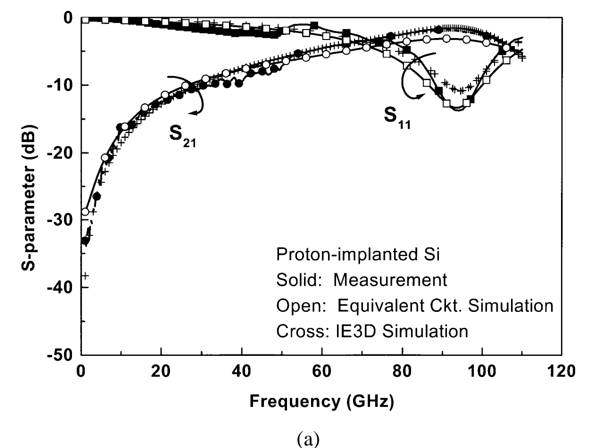

(a)

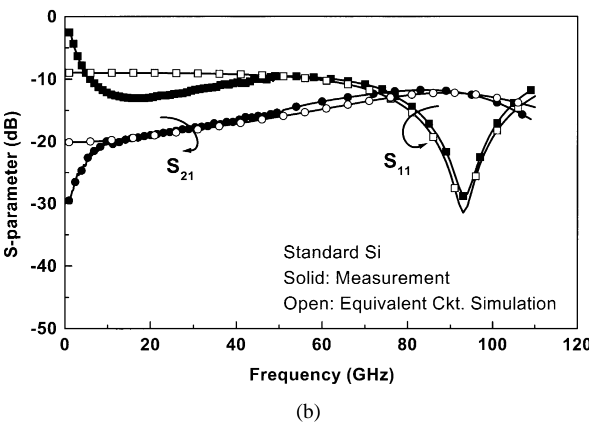

(b)

Fig. 4. Measured and simulated characteristics of a broad-band bandpass filter at 91 GHz fabricated on 1.5-μm SiO_2/Si substrates: (a) with and (b) without the proton implantation. Both ideal *IE3D* designed filter characteristics and equivalent-circuit modeled data are shown for comparison.

B. Bandpass Filter

Fig. 4(a) and (b) compares the RF characteristics of W-band bandpass filters (Fig. 1) for devices with and without the

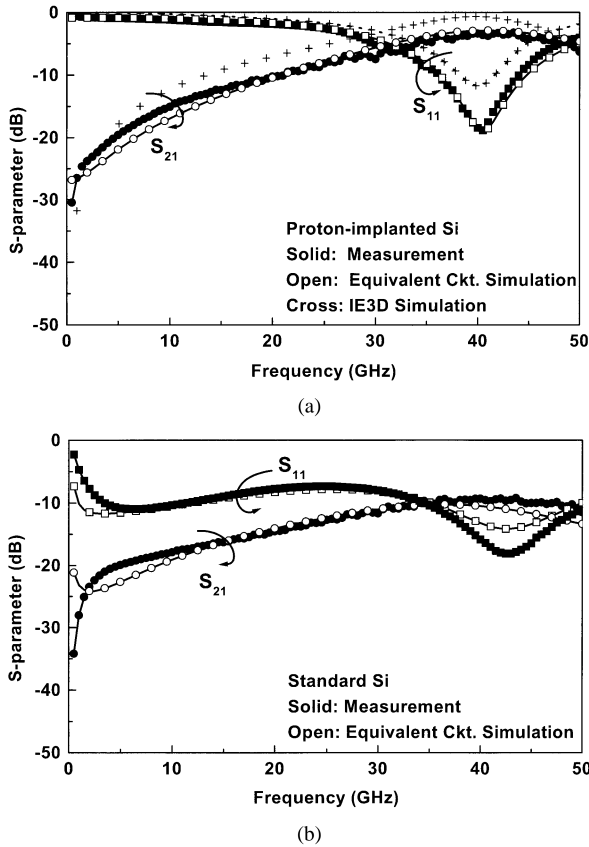

Fig. 5. Measured and simulated 40-GHz bandpass filter characteristics on 1.5-μm SiO_2/Si substrates: (a) with and (b) without proton implantation. Both ideal *IE3D* designed filter characteristics and equivalent-circuit modeled data are shown.

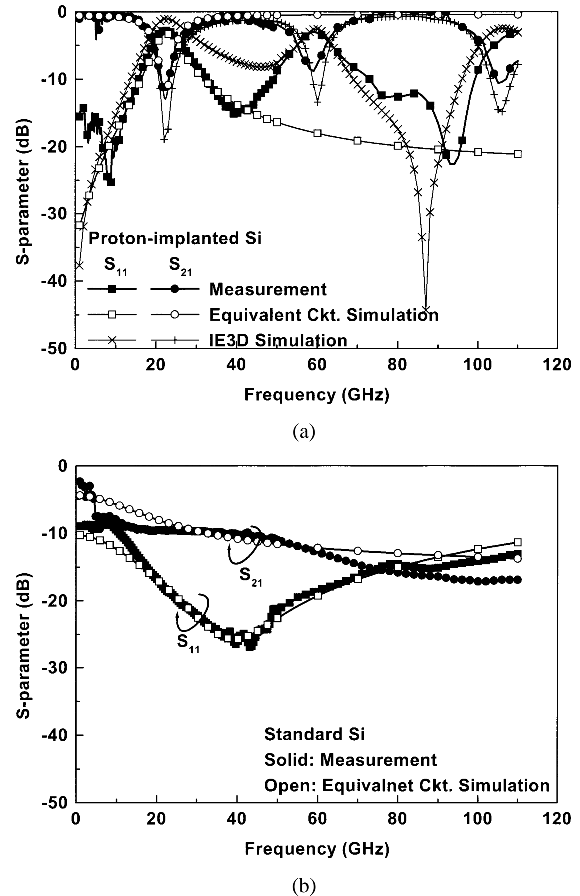

Fig. 6. Measured and simulated characteristics of bandstop filters at 22 GHz on 1.5-μm SiO_2/Si substrates: (a) with and (b) without proton implantation. Both ideal *IE3D* designed filter characteristics and equivalent-circuit modeled data are shown.

optimized proton implantation, respectively. Similar results were obtained for previously published 40-GHz bandpass filters [10] [see Fig. 5(a) and (b)]. The simulations for ideal *IE3D* designed filters are included for comparison. For filters with the proton implantation, excellent RF performance was achieved with only -1.6-dB $S21$ loss at a peak transmission at 91 GHz [see Fig. 4(a)]. This is consistent with the small peak transmission loss of the proton implanted 40 GHz filter, shown in Fig. 5(a). The measured transmission and bandwidth are close to the ideal values. To the best of our knowledge, this is the first demonstration of high-performance filters at W-band on Si substrates, which use a VLSI-compatible process. Poorer peak transmission of -12 dB was measured for the un-implanted filter. This large loss is slightly higher than the -10-dB peak transmission loss for 40 GHz filters shown in Fig. 5(b), which is due to the increased loss at higher frequencies. The -10- to -12-dB loss is greater than the RF gain improvement of MOSFET device scaling down for 2–3 VLSI technology generations [13]. The large return loss, over a wide frequency range, makes these un-implanted filters unacceptable for RF circuit integration.

C. Bandstop Filter

Fig. 6(a) and (b) shows the RF characteristics for 20-GHz bandstop filters on SiO_2/Si substrates and the effects of the proton implantation. The filters are the same type as shown in Fig. 2, but designed at a lower frequency of 20 GHz. The *IE3D* simulation is included in Fig. 6(a) for comparison. Without implantation, there is a large transmission loss from -8 to -17 dB and from 1 to 110 GHz. There is no band rejection at the designed 22-GHz frequency. These poor results show that such bandstop filters are not useful in existing VLSI technology. The opposite is the case for proton-implanted bandstop filters, which display low transmission loss, i.e., only -1.3 and -0.5 dB at 40 and 80 GHz, respectively. The bandstop frequencies at 22, 59, and 105 GHz arise from the odd (1, 3, and 5) harmonic frequencies of the filter, as analyzed by *IE3D* simulation. The results are close to the ideal *IE3D* simulation values.

Fig. 7(a) and (b) compares the RF characteristics of 50-GHz bandstop filters, which have the folded single-end stub structure shown in Fig. 2. Here, again, excellent performance is shown by the proton-implanted stopband filter, but the performance of the standard one is unacceptable.

D. Substrate-Loss Analysis

Here, we describe the use of equivalent-circuit models to analyze and quantize the substrate-loss effects in the studied filters. Fig. 8(a) and (b) shows the physically based equivalent-circuit models for bandpass and bandstop filters, respectively. For bandpass filters, the series $(L_{s1} + L_{s2})C_s$ represents the resonator realized by the coupling lines, and the shunt resistor $R_{\rm sub}$ and capacitor $C_{\rm sub}$ to ground models the Si substrate loss. L_{s1}

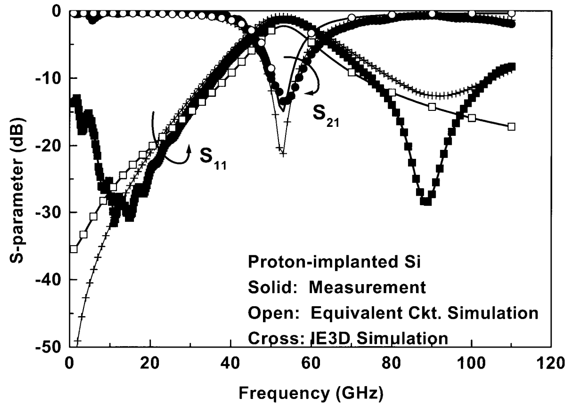

(a)

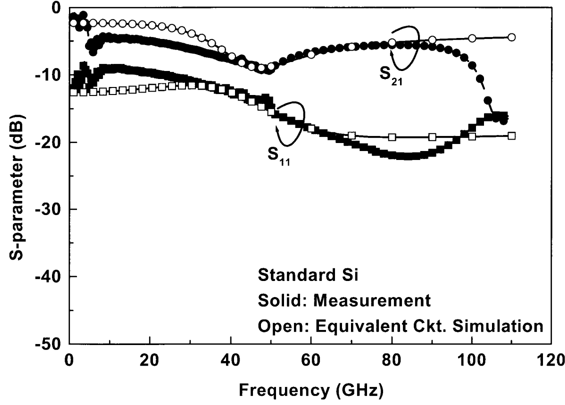

(b)

Fig. 7. Measured and simulated characteristics of bandstop filters at 52 GHz on 1.5-μm SiO_2/Si substrates: (a) with and (b) without proton implantation. Both ideal *IE3D* designed filter characteristics and equivalent-circuit modeled data are shown.

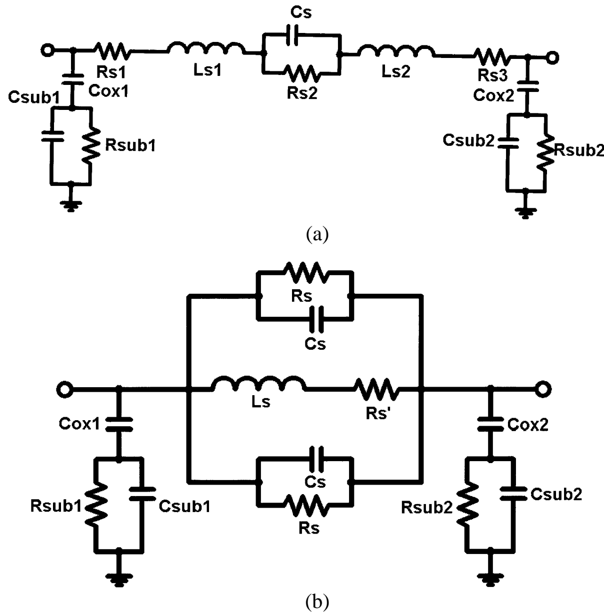

(b)

Fig. 8. Equivalent-circuit models of: (a) bandpass and (b) bandstop filters on Si substrates.

and L_{s2} are the inductance of stubs at the input and output, and the gap capacitance between two ports is expressed as C_s. The series resistors R_{s1} and R_{s3} describe the parasitic resistor loss

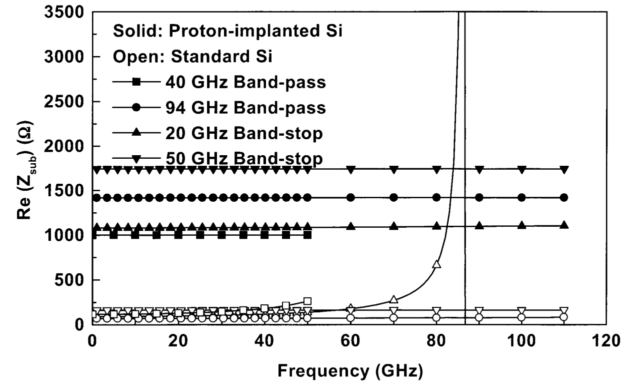

Fig. 9. Magnitude of the substrate impedance extracted using the equivalent-circuit models shown in Fig. 8.

and R_{s2} is the RF loss between coupled structures. As shown in Figs. 4 and 5, good agreement between measured and simulated S_{21}, S_{11}, and bandwidth are obtained at all frequencies for both filter cases. For the bandstop filters, the central conductor is represented as an inductor and the shunt capacitors imitate the two gaps near port 1 [4]. Two resistors are added in parallel with capacitors to model the leakage path of the capacitors on Si. This arises from the substrate loss, as does the shunt resistance and capacitance to ground. Simulated results are also shown in Figs. 6 and 7, and good agreement between measured and modeled S-parameters is obtained. The equivalent circuit can only simulate the first resonance since the lumped-element circuit behaves nonperiodically. Thus, the physically based models are suitable for extraction of the substrate loss.

Fig. 9 shows the magnitude of $|Z_{\rm sub}|$ composed of shunt resistance $R_{\rm sub}$ and capacitance $C_{\rm sub}$, extracted from the equivalent-circuit models in Fig. 8. For conventional filters on Si, the substrate impedances are small, and below 150 Ω over the whole frequency range. The difference in $Z_{\rm sub}$ for filters designed at different frequencies results from the different filter sizes. For un-implanted bandpass filters, the small shunt impedance to ground explains the poor peak transmission and large return loss. Also, the small $|Z_{\rm sub}|$ in the un-implanted bandstop filters is consistent with the large return loss and poor band rejection. In contrast, the implanted filters show substrate impedances $\sim$10$\times$ larger at $>$1000 Ω—this greatly reduces the loss for RF devices.

IV. Conclusion

We have described good RF performance over the range from 22 to 91 GHz for both bandpass and bandstop microwave coplanar filters fabricated on Si substrates that have undergone an optimized proton implantation process. The excellent RF performance is close to *IE3D* simulated characteristics. In contrast, much poorer filter characteristics were measured for un-implanted filter devices. Here, the substrate impedance was found to be the major cause of the poor filter performance, as determined by equivalent-circuit model analysis. The modified proton implantation scheme, compatible with current VLSI technology and applied after whole wafer processing, has great potential for integrating microwave filters into MMICs on Si substrates where the cost and size can be optimized.

ACKNOWLEDGMENT

The authors would like to thank D. C. Nio, National Chung-Shen Science Research Institute, Tawain, R.O.C., for help with the RF measurements.

REFERENCES

[1] A. Takacs, H. Aubert, P. Pons, R. Plana, T. Parra, J. Graffeuil, H. Baudrand, and J. L. Cazaux, "An original micromachined planar Ka band filter based on a resonant coupling irises topology," in *IEEE Int. Semiconductor Conf.*, 2001, pp. 147–150.

[2] T. M. Weller and L. P. Katehi, "Miniature stub and filter designs using the microshield transmission line," in *IEEE MTT-S Int. Microwave Symp. Dig. Dig.*, vol. 2, June 1995, pp. 675–678.

[3] J. Papapolymerou and G. E. Ponchak, "Microwave filters on a low resistivity Si substrate with a polyimide interface layer for wireless circuits," in *IEEE RF-IC Symp. Dig.*, June 2001, pp. 125–128.

[4] K. Hettak, N. Did, A.-F. Sheta, and S. Toutain, "A class of novel uniplanar series resonators and their implementation in original applications," *IEEE Trans. Microwave Theory Tech.*, vol. 46, pp. 1270–1276, Sept. 1998.

[5] A. Chin, K. Lee, B. C. Lin, and S. Horng, "Picosecond photoresponse of carriers in Si ion-implanted Si," *Appl. Phys. Lett.*, vol. 69, pp. 653–655, 1996.

[6] Y. H. Wu, A. Chin, K. H. Shih, C. C. Wu, C. P. Liao, S. C. Pai, and C. C. Chi, "Fabrication of very high resistivity Si with low loss and cross talk," *IEEE Electron Device Lett.*, vol. 21, pp. 442–444, Sept. 2000.

[7] Y. H. Wu, A. Chin, K. H. Shih, C. C. Wu, S. C. Pai, C. C. Chi, and C. P. Liao, "RF loss and cross talk on extremely high resistivity (10 K–1 MΩ − cm) Si fabricated by ion implantation," in *IEEE MTT-S Int. Microwave Symp. Dig.*, June 2000, pp. 221–224.

[8] K. T. Chan, A. Chin, C. M. Kwei, D. T. Shien, and W. J. Lin, "Transmission line noise from standard and proton-implanted Si," in *IEEE MTT-S Int. Microwave Symp. Dig.*, June 2001, pp. 763–766.

[9] K. T. Chan, A. Chin, Y. B. Chan, T. S. Duh, and W. J. Lin, "Integrated antenna on Si, proton-implanted Si and Si-on-quartz," in *Int. Electron Devices Meeting Tech. Dig.*, Dec. 2001, pp. 903–906.

[10] K. T. Chan, C. Y. Chen, A.Albert Chin, J. C. Hsieh, J. Liu, T. S. Duh, and W. J. Lin, "40-GHz coplanar waveguide bandpass filters on silicon substrate," *IEEE Microwave Wireless Comp. Lett.*, pp. 429–431, Nov. 2002.

[11] C. M. Nam and Y. S. Kwon, "Coplanar waveguides on silicon substrate with thick oxidized porous silicon (OPS) layer," *IEEE Microwave Guided Wave Lett.*, vol. 8, pp. 369–371, Nov. 1998.

[12] K. J. Herrick, T. A. Schwarz, and L. P. B. Kathehi, "Si-micromachined coplanar waveguides for use in high-frequency circuits," *IEEE Trans. Microwave Theory Tech.*, vol. 46, pp. 762–768, June 1998.

[13] Y. H. Wu, A. Chin, C. S. Liang, and C. C. Wu, "The performance limiting factors as RF MOSFET's scaling down," in *IEEE RF-IC Symp. Dig.*, June 2000, pp. 151–154.

K. T. Chan was born in Hsinchu, Taiwan, R.O.C., in 1977. She received the B.S. and M.S. degrees in electronic engineering from the National Chiao-Tung University, Hsinchu, Taiwan, R.O.C., in 1999 and 2000, respectively, and is currently working toward the Ph.D. degree at the National Chiao-Tung University.

Her research interest includes Si RF devices and technologies.

Albert Chin (SM'94) received the Ph.D. degree in electrical engineering from The University of Michigan at Ann Arbor, in 1989.

He then joined AT&T Bell Laboratories, General Electric-Electronic Laboratory, and then visited Texas Instruments Incorporated. He possesses five years industrial experience within the U.S. He has authored or coauthored over 150 technical papers and presentations. His technical background includes III–V's, Si VLSI, and RF devices. He developed the resonant cavity photodetector, high-mobility strain-compensated pseudomorphic high electron-mobility transistor (pHEMT) and high-κ Al_2O_3 and La_2O_3 gate dielectrics on Si. He is also a pioneer of very high-resistivity Si research using ion implantation in 1996, and much improved RF loss and noise close to GaAs has been realized up to 100 GHz. He is currently involved with RF, memory, and defect-free SiGe technologies.

Ming-Fu Li (M'91–SM'99) received the B.S. degree in physics from Fudan University, Shanghai, China, in 1960.

He then joined the University of Science and Technology of China, and became a Professor in 1986. He was a Visiting Scholar with University of Illinois at Urbana-Champaign (1979–1981), and the University of California at Berkeley (1986–1987, 1990–1991). In 1991, he joined the Electrical and Computer Engineering Department, National University of Singapore, Singapore, and became a Professor in 1996. He has authored or coauthored over 200 research papers and two books. His current research interests are in the areas of deep sub-micrometer CMOS device technology, reliability, quantum modeling, and analog IC design.

Prof. Li has served on several International Program Committees and Advisory Committees in international semiconductor conferences.

Dim-Lee Kwong (A'84–SM'90), photograph and biography not available at time of publication.

Sean P. McAlister (SM'02) was born in Durban, South Africa. He received the M.Sc. degree from the University of Natal, Natal, South Africa, in 1968, and the Ph.D. degree in physics from Cambridge University, Cambridge, U.K., in 1971.

Following four years with Simon Fraser University, Vancouver, BC, Canada, he joined the National Research Council of Canada, Ottawa, ON, Canada, in 1975. He has been involved in the fields of low-temperature physics, magnetism, and semiconductor materials. He is a Principal Research Officer with the Institute for Microstructural Sciences and leads the efforts in device physics. His interests are in the design, simulation, and characterization of heterostructure devices.

D. S. Duh, photograph and biography not available at time of publication.

W. J. Lin, photograph and biography not available at time of publication.

C. Y. Chang, photograph and biography not available at time of publication.